Compact Model of Single TeraFET Spectrometer

I.Gorbenko[1)], V. Kachorovskii[1,2)], M. Shur[2)]

[1)] Ioffe Institute, Sankt Petersburg, 194021, Russia

[2)] Rensselaer Polytechnic Institute Troy, NY 12180, USA

11th International MOS-AK Workshop

(co-located with the IEDM and CMC Meetings)

Silicon Valley, December 5, 2018

Outline

- Motivation
- Plasmonic Detectors Controlled by Phase Asymmetry $\longrightarrow$ resonant TeraFETs
  - Basic Equations
  - Results and Discussion
- Conclusions

THz Ranges and Applications

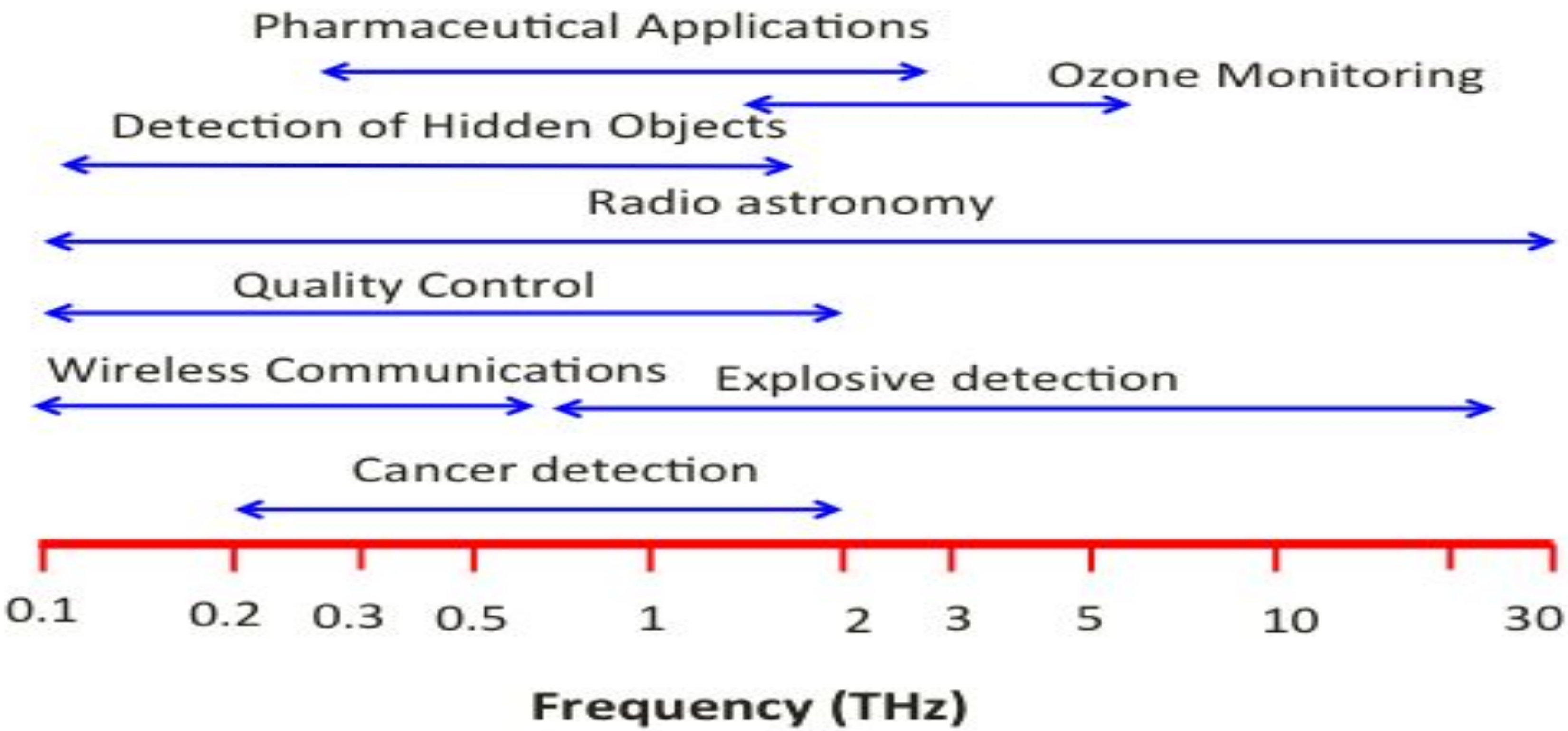

Si and SiGe range

From T. Otsuji and M.S. Shur, Terahertz Plasmonics. Good results and great expectations, IEEE Microwave Journal October 2014

From 1G to Beyond 5G WIFI

- 1G 0.8 GHz
- 3G 1.8 to 2.5 GHz
- 4G 2 to 8 GHz (2012-2018)
- 5G 1 to 28 GHz (2019-2020)
- <u>Beyond 5G</u> <u>1 to 1,000 GHz</u> <u>(2020-2025)</u>

How could FET technology support Beyond 5G?

SAMSUNG ,TSMC, Global foundry 7 nm: 20-30 percent higher performance, 30-50 percent less power, 40% shrink compared to 10 nm

- SAMSUNG 7 nm 27 nm fin pitch 54 nm gate pitch
  - 256Mb SRAM test chips and application processor (six-core GPU)
- TSMC 7nm
  - Mobile and network processors, CPUs, graphics processors, FPGAs, and AI accelerators
- Gate All Around 3 nm

22, 14, 10, 7 nm, 3nm Gate All around planned

22 nm FIN technology

10 nm FIN technology

14 nm FIN technology

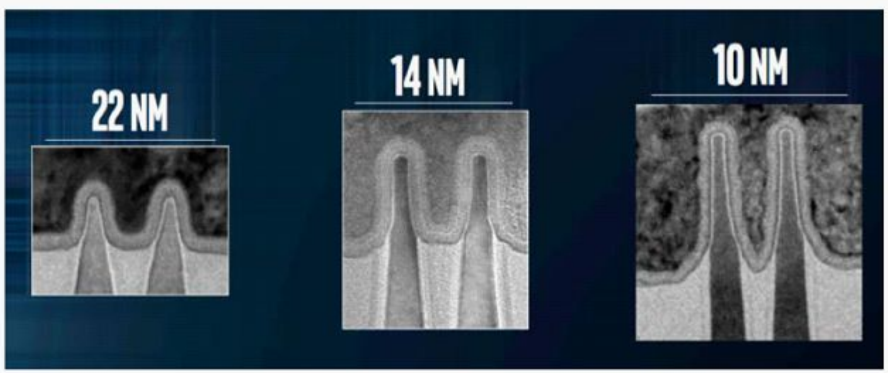

Image: Intel

DARPA Electronics Resurgence Initiative

- **The U.S. Defense Advanced Research Projects Agency is launching a huge expansion of its Electronics Resurgence Initiative, boosting the program to US $1.5 billion over five years.**

- **One of the thrusts is stated as " What can you do with older manufacturing nodes (like 90 nanometers) to make them competitive with 5-nm or 7-nm design?"**

Even longer channel Si CMOS and Si/SiGe BiCMOS operate in THz range?

Mean Free Path in Silicon Inversion Layers

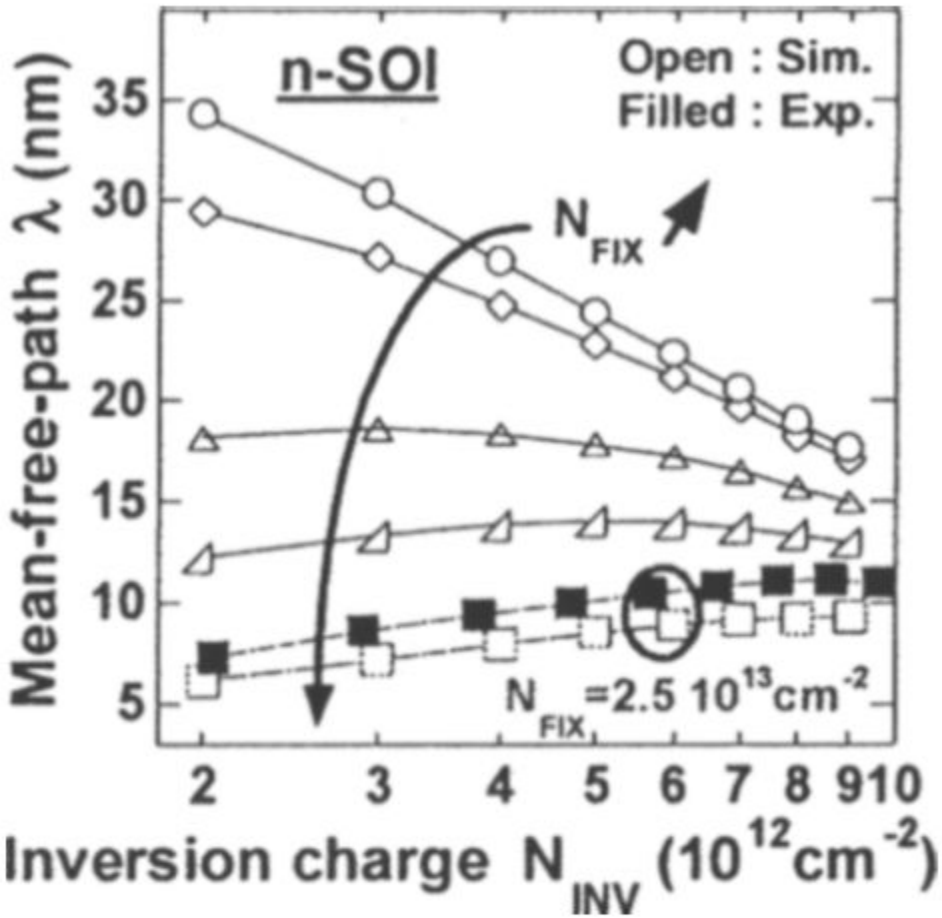

v. Barral'r', T. Poiroux', S. Barraud', O. Bonne', F. Andrieu', C. Buj-Dufournet', L. Brevard', D. Lafond', O. Faynot', D. Munteanu', J.L. Autrarr' and S. Deleonibus, Electron Mean-Free-Path Experimental Extraction on Ultra-Thin and Ultra-Short Strained and Unstrained FDSOI n-MOSFETs ieeexplore.ieee.org/iel5/5406683/5418382/05418445.pdf

Ballistic mobility in Si: proportional to length (A. Kastalski and M. Shur, 1981)

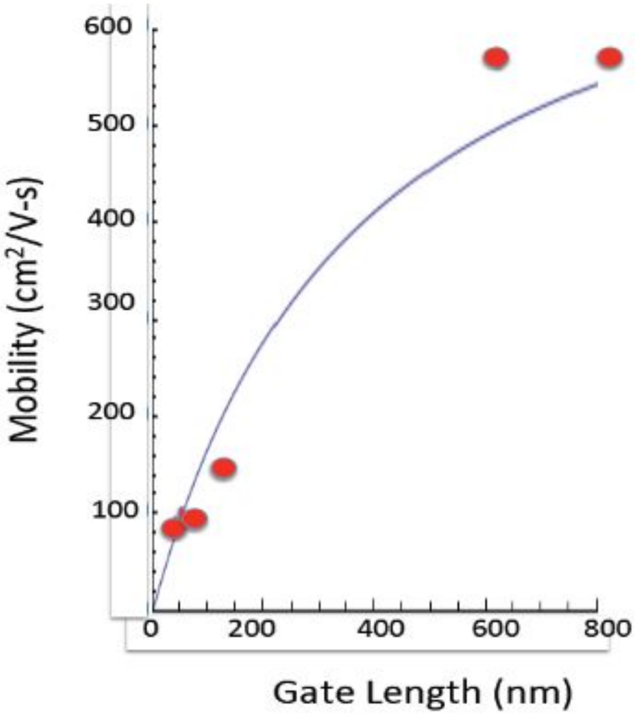

Data from W. Knap, F. Teppe, Y. Meziani, N. Dyakonova, J. Lusakowski, F. Bouef, T. Skotnicki, D. Maude, S. Rumyantsev and M. S. Shur, Appl. Phys. Lett, Vol. 85, No 4, pp. 675-677 (2004)

$$1/\mu_{eff} = 1/\mu + 1/\mu_{bal}$$

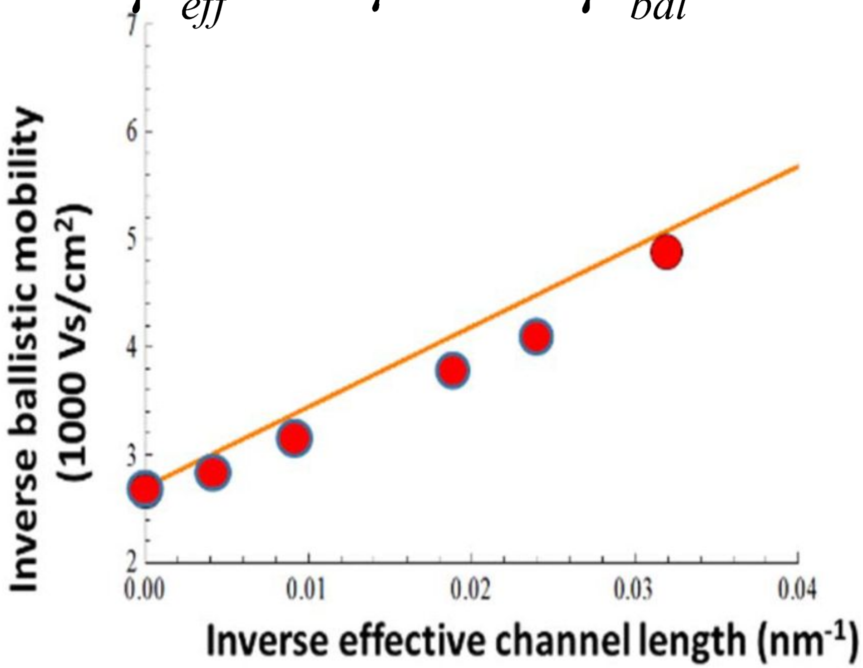

D. Antoniadis, IEEE Transactions on Electron Dev. Vol. 63, No 7, pp. 2650 – 2656 (2016)

Effective mobility for InGaAs and Si versus gate length

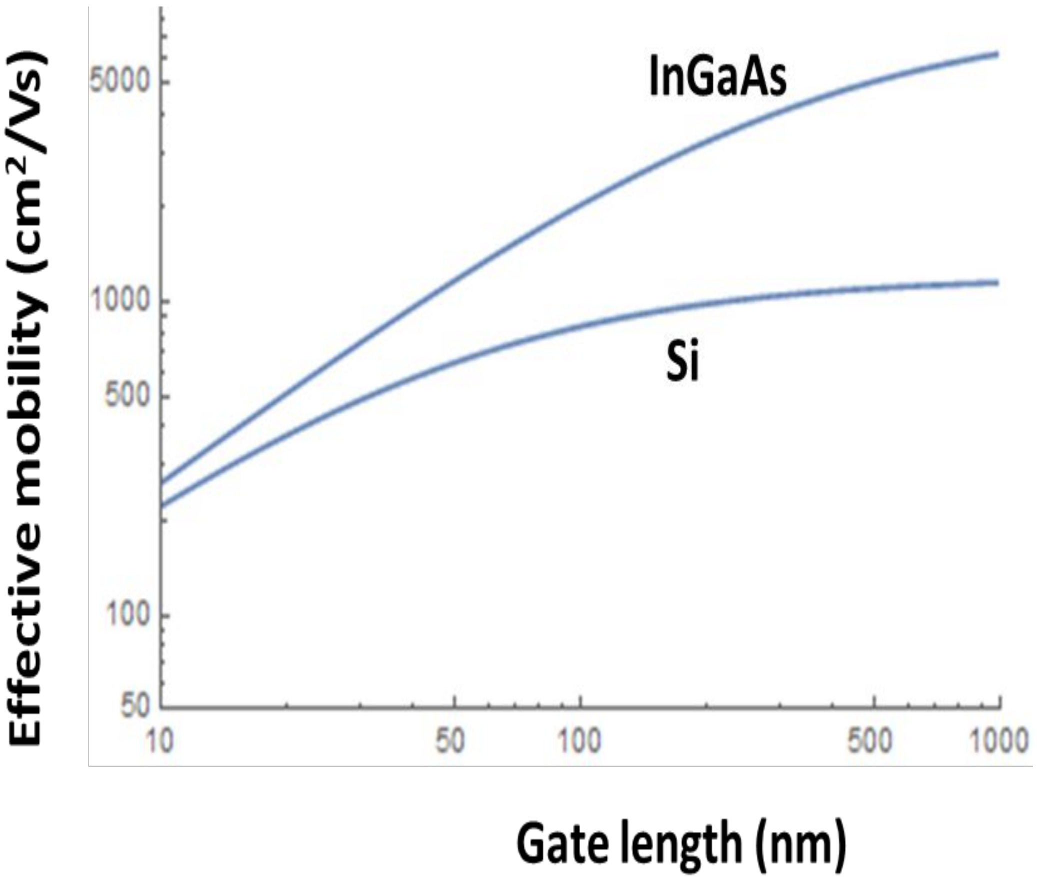

Parameters used in the calculation: the silicon effective mass 0.19; InGaAs effective mass 0.041, $n_s = 2\times10^{16}$ m^2, room temperature electron mobility 1200 cm^2/Vs and 8500 cm^2/Vs for Si and InGaAs, respectively.

Maximum Modulation Frequency of Si MOS

S
i

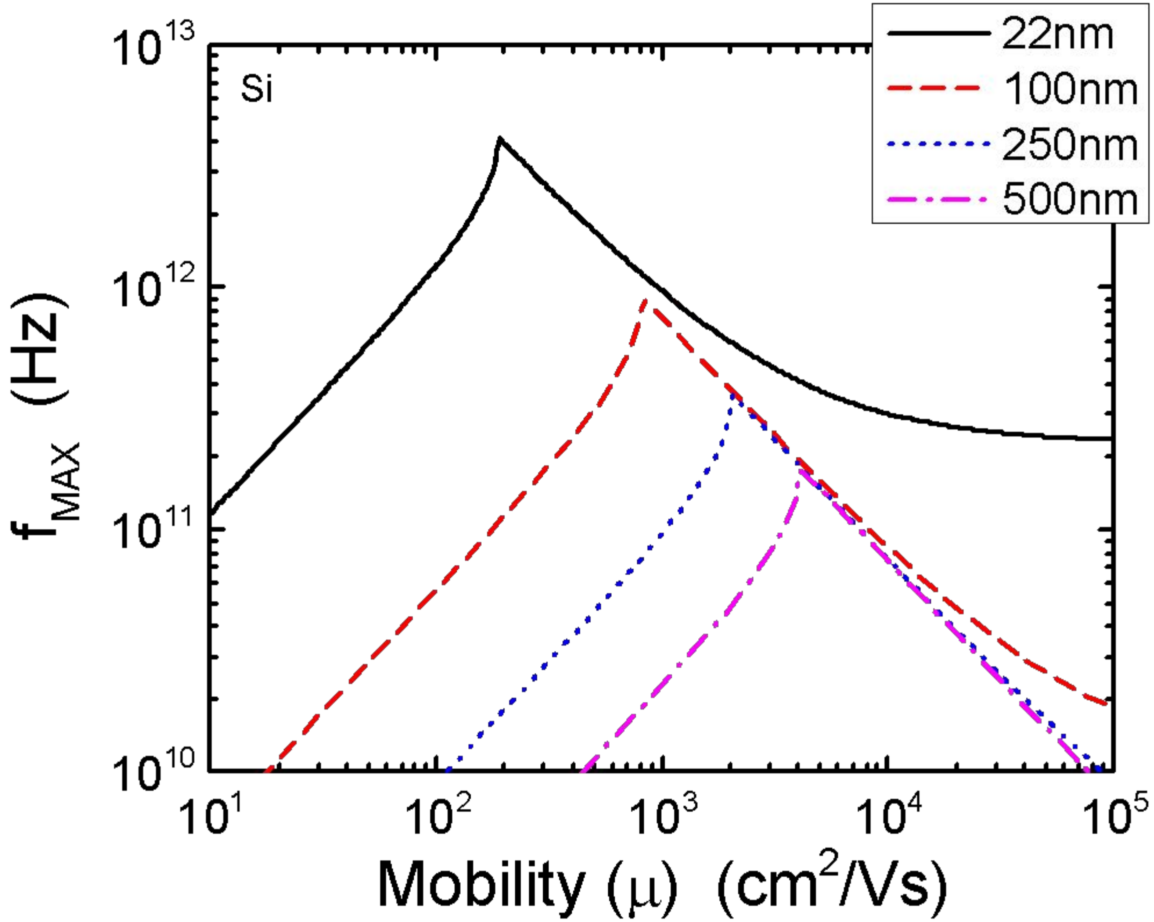

"Response of Plasmonic Terahertz Detectors to Amplitude Modulated Signals", Solid-State Electronics 111, Pages 76-79; **G. Rupper, S. Rudin, and M. Shur.**

Response of field effect transistor and plasma crystal to the THz radiation

Plasma wave terahertz electronics

Plasma waves can propagate much faster than electrons: $s \sim 10^8\ cm/s$

Channel of FET plays a role of a resonant cavity for plasma waves. Resonant frequency can be tuned by gate voltage: $\omega_0 = \pi s / 2L \propto \sqrt{U_g}$

Nonlinearity of plasma waves can be used for ***THz detection***. Response is proportional to radiation power: $\delta U \propto P$

Dc current in the channel excites plasma waves ⟹ ***THz emission***

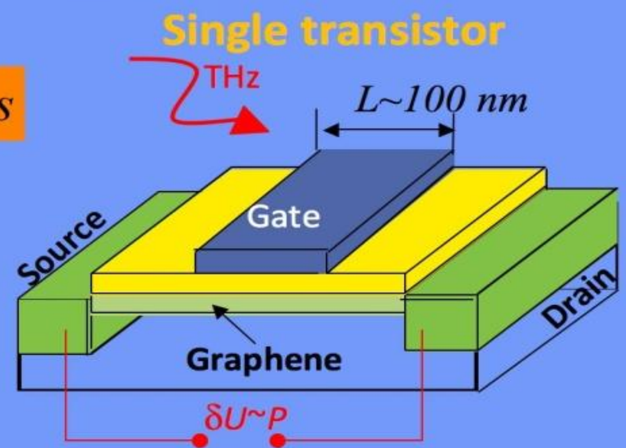

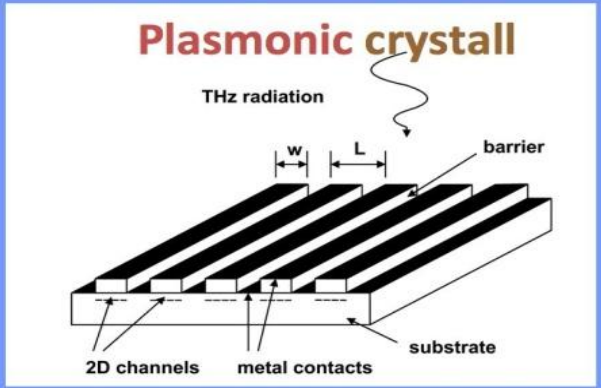

Rectification of plasma waves enables THz detection

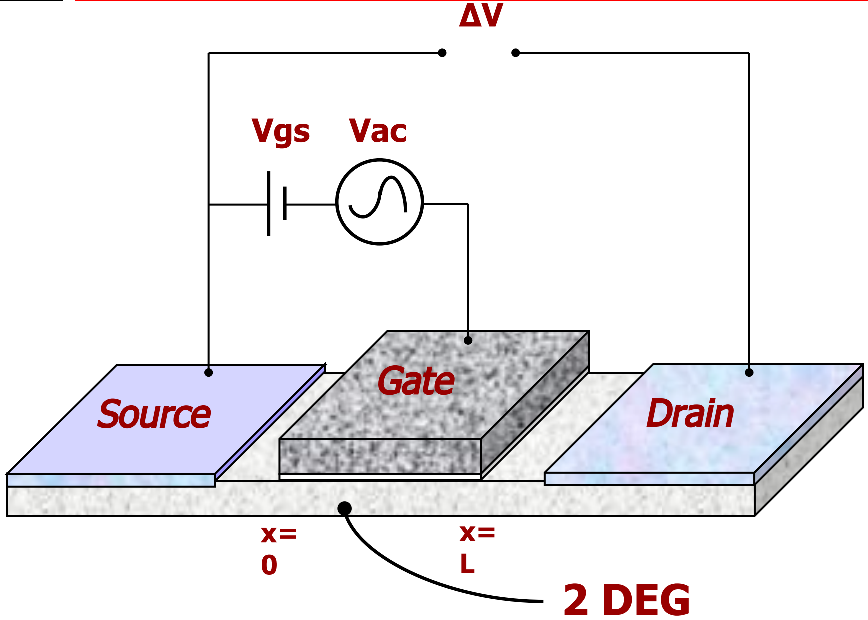

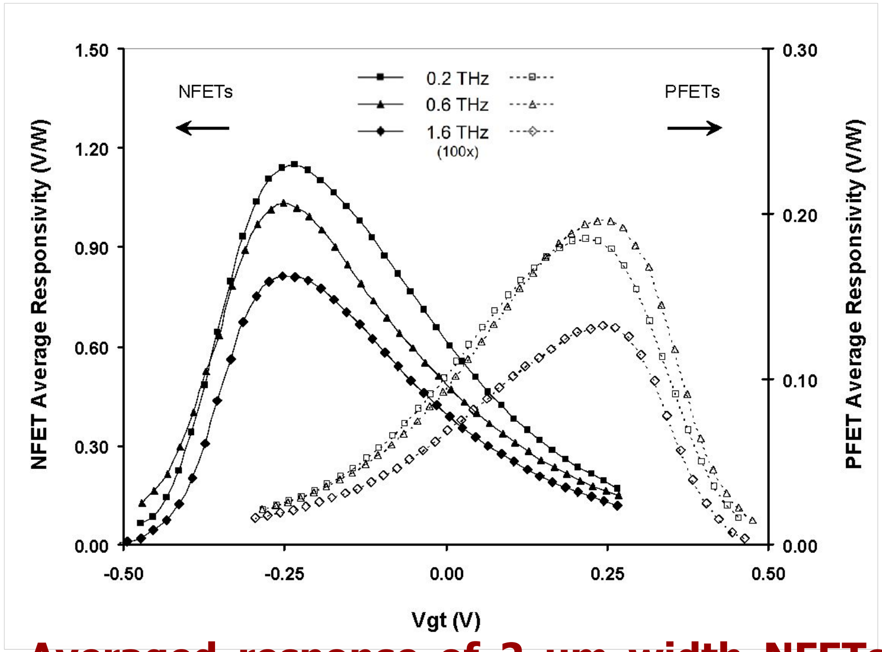

Conceptual schematic of FET terahertz response. Vac is the induced voltage resulting from the incident beam; ΔV is the proportional drain voltage response.

Averaged response of 2 µm width NFETs and 5 µm PFETs at 0.2, 0.6 and 1.6 THz illustrating broad range complementary behavior.

After: M. Dyakonov and M. Shur, "Detection, mixing, and frequency multiplication of terahertz radiation by two-dimensional electronic fluid," IEEE Transactions on Electron Devices, vol. 43, pp. 380-387, 1996.

Source: **W. Stillman, F. Guarin, V. Y. Kachorovskii, N. Pala, S. Rumyantsev, M. S. Shur, and D. Veksler, "Nanometer scale complementary silicon MOSFETs as detectors of terahertz and sub-terahertz radiation," Atlanta, GA, USA, 2007.**

Quality factors for gated Si MOS region

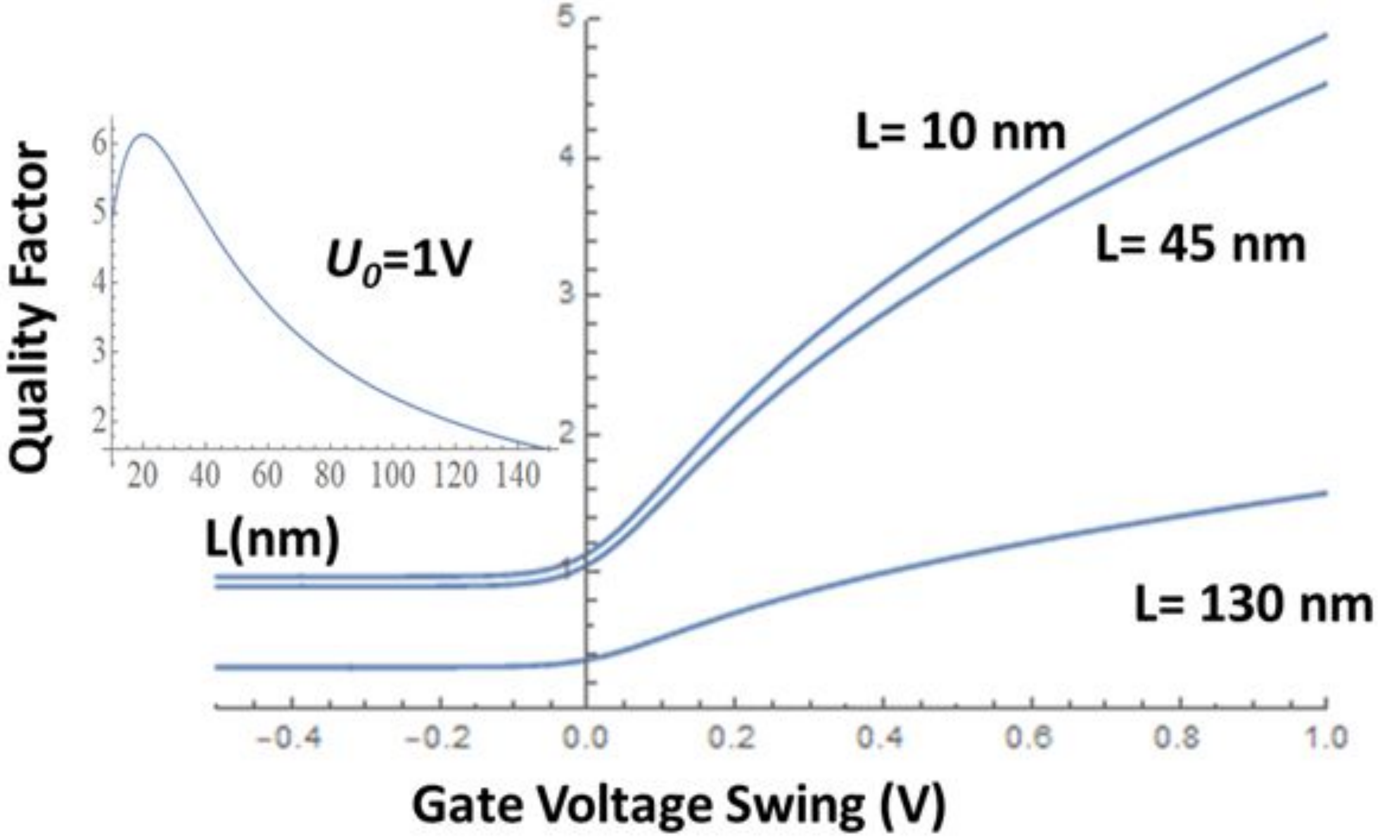

FinFET Response to 0.2 THz

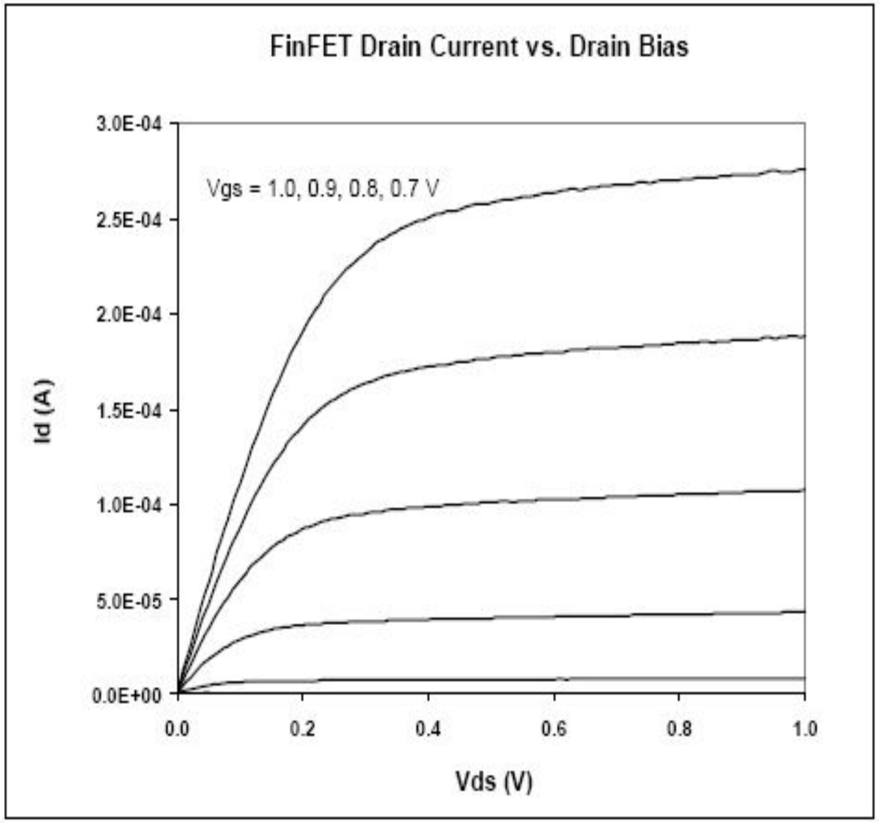

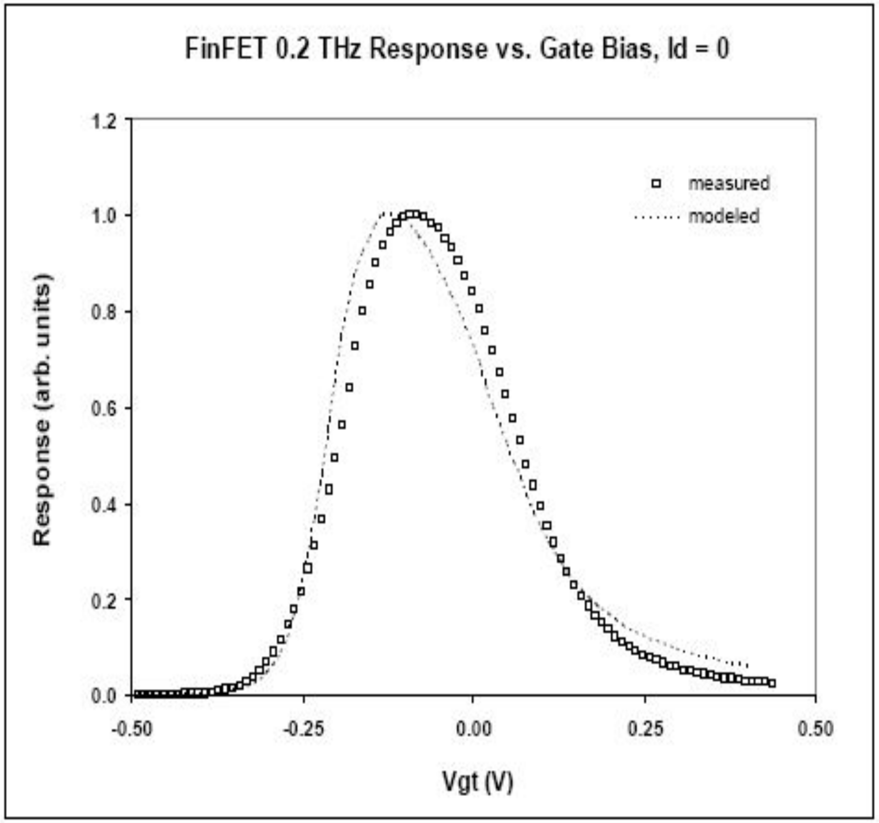

W. Stillman, C. Donais, S. Rumyantsev, M. Shur, D. Veksler, C. Hobbs, C. Smith, G. Bersuker, W. Taylor and R. Jammy, Silicon FIN FETs as detectors of terahertz and sub-terahertz radiation, International Journal of High Speed Electronics and Systems, vol. 20, No. 1, pp. 27-42 March (2011)

Silicon CMOS Plasmonic detectors work up to 5 THz

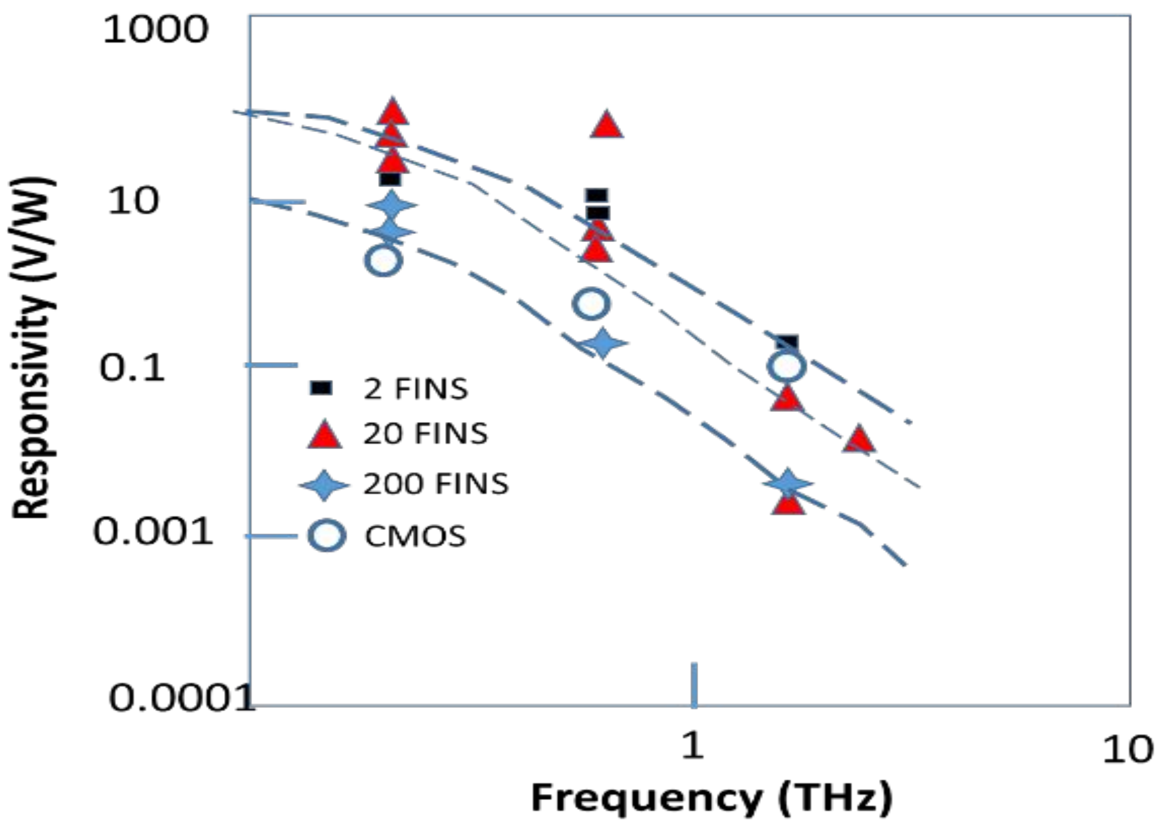

After W. Stillman, C. Donais, S. Rumyantsev, M. Shur, D. Veksler, C. Hobbs, C. Smith, G. Bersuker,

W. Taylor and R. Jammy, Silicon FIN FETs as detectors of terahertz and sub-terahertz radiation,

International Journal of High Speed Electronics and Systems, vol. 20, No. 1, pp. 27-42 March

THz compact model is required for THz design

AIM-Spice new models

- HBT
- MOSFET and SOI (5 new models , *n*- and *p*-channel)
- MESFET (2 new models)
- HFET model
- a-Si TFT and poly TFT models
- THz HFET and CMOS (under development)
- TeraFET Spectrometer – THIS WORK

Unified Charge Control Model

$$n_s = n_o \ln\left[1 + \exp\left(\frac{V_{GT} - \alpha V_F}{\eta V_{th}}\right)\right]$$

where the carrier sheet density at threshold is given by

$$n_o = \frac{\eta V_{th} c_i}{q}$$

(After T. A. Fjeldly, T. Ytterdal, and M. S. Shur
Introduction to Device Modeling and Circuit Simulation,
Wiley, New York (1998), Section 6.3)

THz SPICE

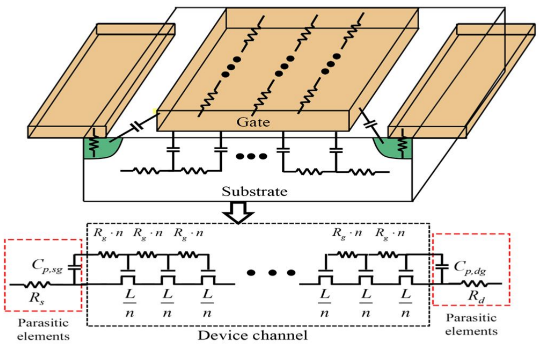

THz SPICE versus Traditional SPICE

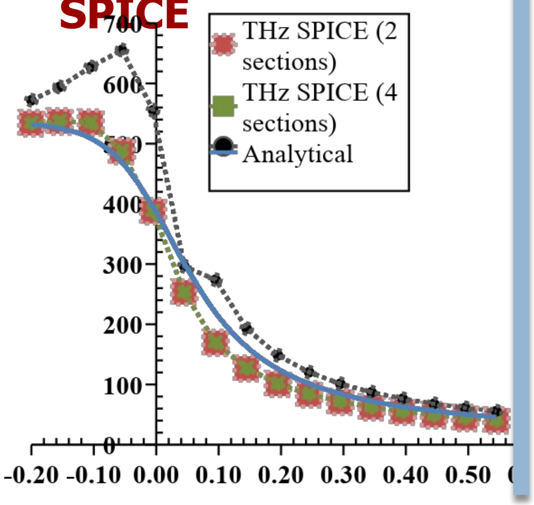

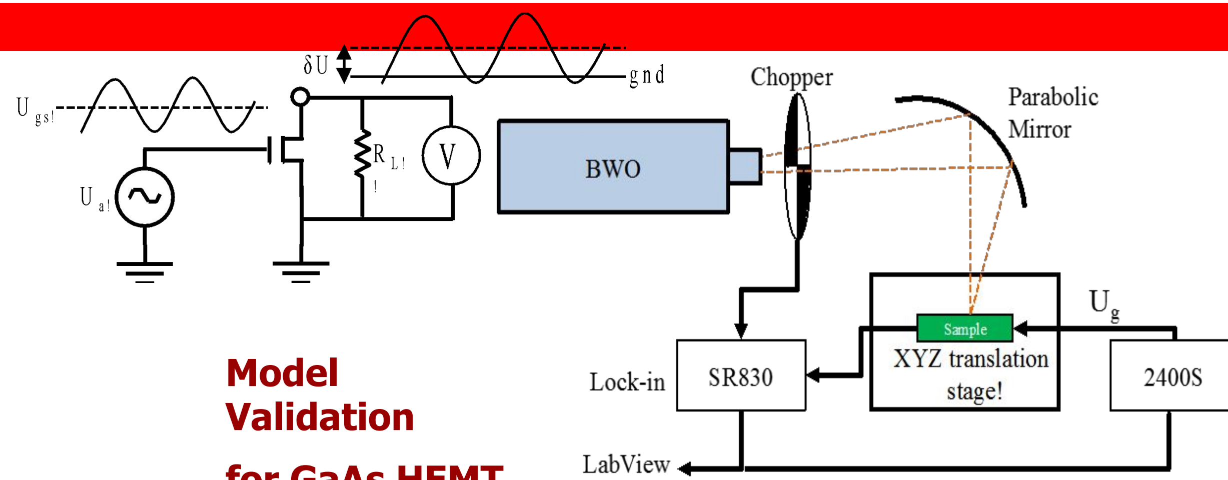

Model Validation for GaAs HEMT

Simulated Si NMOS response for at 200 GHz

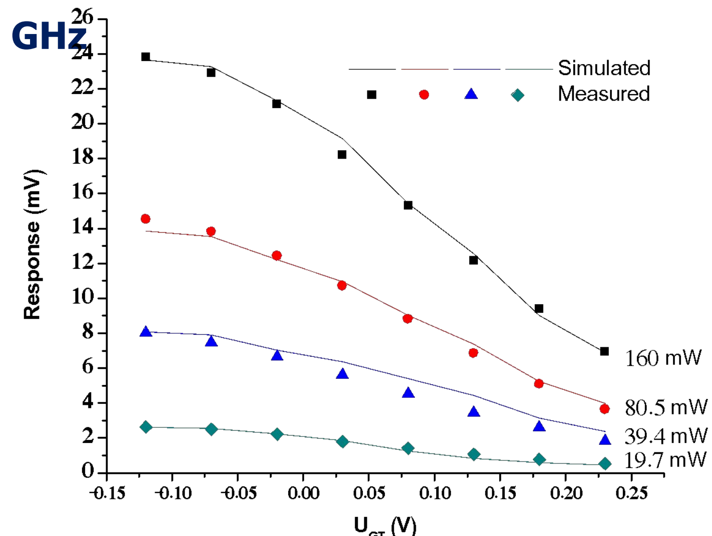

M. Shur. Terahertz Compact SPICE Model, (Invited) 2016 MIXDES-23rd International Conference Mixed Design of Integrated Circuits and Systems, 23-25 June 2016, Page(s): 27 – 31, ISBN: 978-83-63578-08-4.

AIM-SPICE MOSFET model

IBM Sub-0.1 µm process, L_{eff} = 0.09 µm

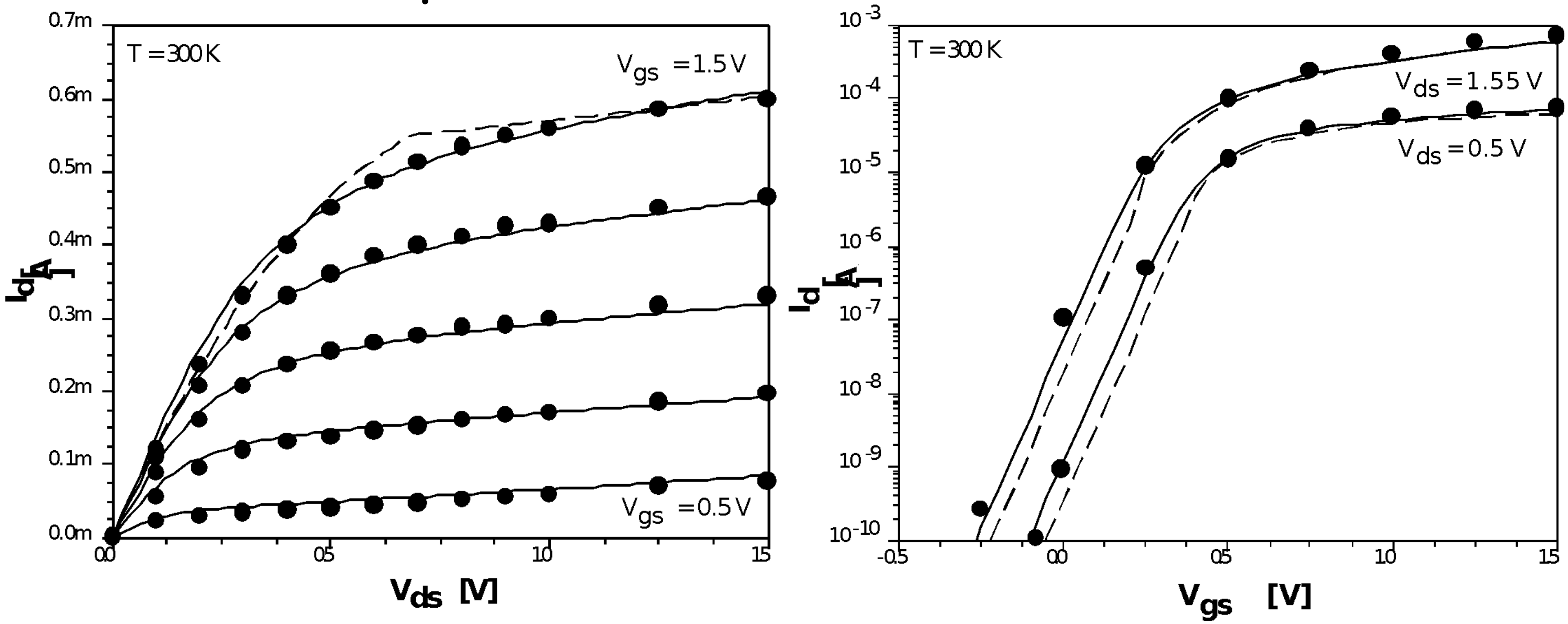

Simulated (solid lines) and measured (dots) I-V characteristics. The dashed

lines are simulated characteristics using the SPICE MOSFET level 3 model

Rectification of plasma waves requires asymmetry between source and drain

Radiation amplitude U_a is fixed at source, current fixed at drain

$$V_{dc} \propto U_a^2$$

Radiation amplitudes U_a and U_b fixed at source and drain

$$V_{dc} \propto U_a^2 - U_b^2$$

Radiation has equal amplitudes at source and drain but phase–shifted by θ

$$V_{dc} \propto U_a^2 \sin\theta$$

phase-sensitive spectroscopy

Plasmonic Detectors Controlled by Phase Asymmetry → resonant TeraFETs

Circularly-polarized radiation

Top view

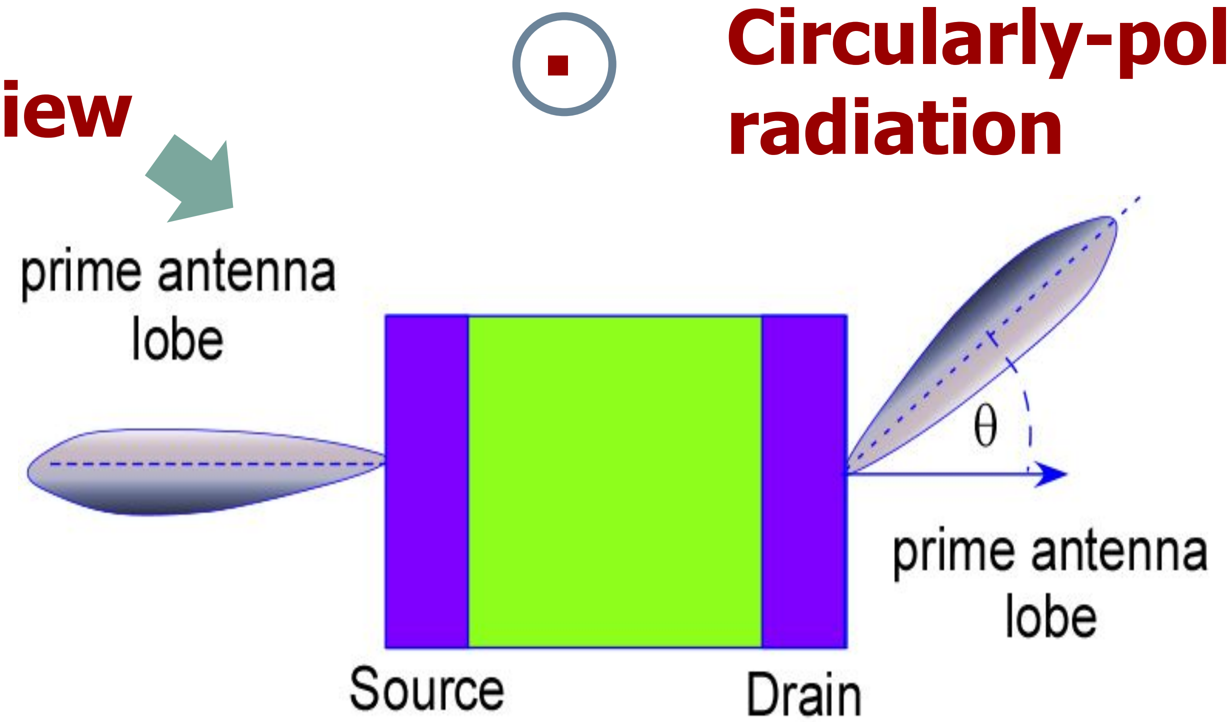

Phase Asymmetry imposed by BC

$$U(0) = U_g + U_a \cos(\omega t + \theta),$$
$$U(L) = U_g + V + U_b \cos(\omega t).$$

direction of dc current is determined by phase shift

Phase Asymmetry induced by nonzero incident angle of incoming radiation

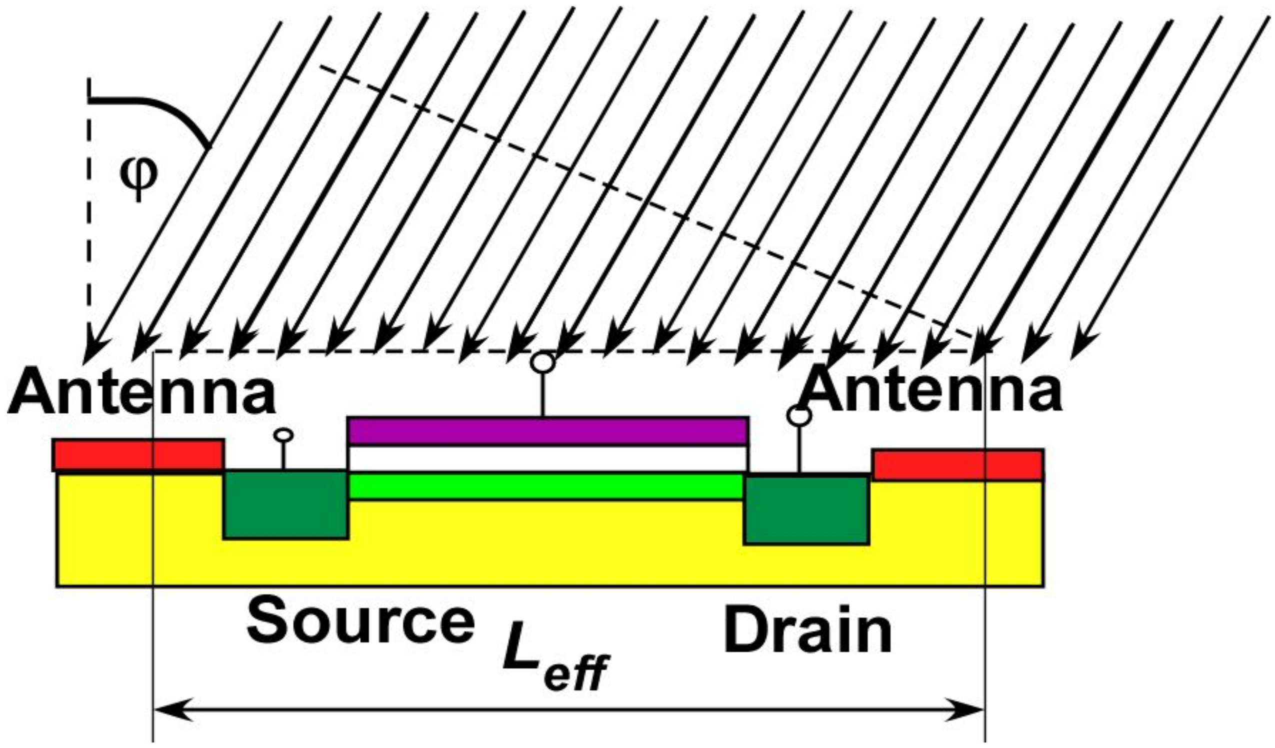

Hydrodynamics of plasma waves

$$\begin{cases} \dfrac{\partial v}{\partial t} + v\dfrac{\partial v}{\partial x} + \gamma v = -\dfrac{e}{m}\dfrac{\partial U}{\partial x}, \\ \dfrac{\partial U}{\partial t} + \dfrac{\partial (Uv)}{\partial x} = 0. \end{cases}$$

Navier-Stokes equation

Continuity equation

$$n(\mathrm{x}) = \frac{CU(\mathrm{x})}{e}$$

Gradual channel approximation

$$U(0) = U_g + U_a \cos(\omega t + \theta),$$
$$U(L) = U_g + V + U_b \cos(\omega t).$$

Boundary conditions

Rectification of plasma waves

$$\begin{cases} \dfrac{\partial v}{\partial t} + v\dfrac{\partial v}{\partial x} + \gamma v = -\dfrac{e}{m}\dfrac{\partial U}{\partial x}, \\ \dfrac{\partial U}{\partial t} + \dfrac{\partial (Uv)}{\partial x} = 0. \end{cases}$$

nonlinear terms

$$n = n_0(x) + \left[n_1(x)e^{-i\omega t} + n_{-1}(x)e^{i\omega t}\right]/2 + \cdots,$$

$$v = v_0(x) + \left[v_1(x)e^{-i\omega t} + v_{-1}(x)e^{i\omega t}\right]/2 + \cdots$$

rectification

$$\frac{V_{dc}}{U_g} = \frac{\gamma}{4s^2}\int_0^L dx\left(n_1 v_{-1} + n_{-1}v_1 - \frac{d[v_1(x)v_{-1}(x)]}{\gamma\, dx}\right)$$

Final result

$$V = \frac{\omega}{\sqrt{\omega^2+\gamma^2}} \frac{\alpha\left(U_a^2 - U_b^2\right) + \beta U_a U_b \sin\theta}{4U_g|\sin(kL)|^2}$$

$$\alpha = \left(1 + \frac{\gamma\Omega}{\Gamma\omega}\right)\sinh^2\left(\frac{\Gamma L}{s}\right) - \left(1 - \frac{\Gamma\gamma}{\Omega\omega}\right)\sin^2\left(\frac{\Omega L}{s}\right),$$

$$\beta = 8\sinh\left(\frac{\Gamma L}{s}\right)\sin\left(\frac{\Omega L}{s}\right)$$

$$k = \left(\Omega + i\Gamma\right)/s \qquad \Omega = \sqrt{\frac{\sqrt{\omega^4+\omega^2\gamma^2}}{2} + \frac{\omega^2}{2}};\ \Gamma = \sqrt{\frac{\sqrt{\omega^4+\omega^2\gamma^2}}{2} - \frac{\omega^2}{2}}$$

Response is nonzero for U_a=U_b → dc response induced by phase-asymmetry

$$V = \frac{\beta \omega U_a^2 \sin\theta}{4U_g \left|\sin(kL)\right|^2 \sqrt{\omega^2 + \gamma^2}}$$

$$k = \left(\Omega + i\Gamma\right)/s$$

$$\Omega = \sqrt{\frac{\sqrt{\omega^4 + \omega^2\gamma^2}}{2} + \frac{\omega^2}{2}};\ \Gamma = \sqrt{\frac{\sqrt{\omega^4 + \omega^2\gamma^2}}{2} - \frac{\omega^2}{2}}$$

$$\beta = 8\sinh\left(\frac{\Gamma L}{s}\right)\sin\left(\frac{\Omega L}{s}\right)$$

General diagram illustrating different regimes of TeraFET operation

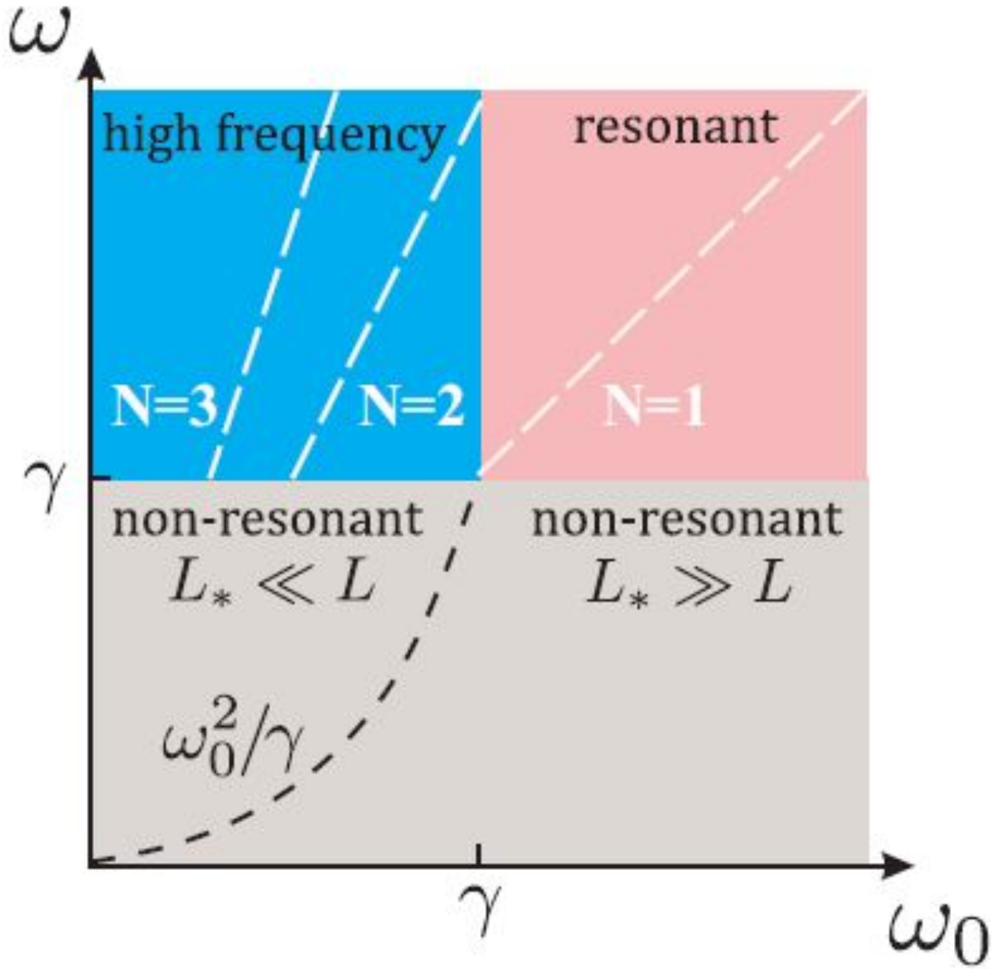

Limiting cases: resonant case

$\omega \gg \gamma, \omega_0 \gg \gamma$ where

$$\omega_0 = \frac{\pi s}{L}$$

fundamental plasma frequency

In vicinity of resonances $\omega \approx \omega_0$: $\delta\omega = \omega - \omega_0$

$$V(\delta\omega) = \frac{\left(U_a{}^2 - U_b{}^2\right)(3\gamma^2/4 - \delta\omega^2) + 4U_a U_b (-1)^N \delta\omega\gamma \sin\theta}{4U_g(\delta\omega^2 + \gamma^2/4)}$$

Resonance dependence of dc response at a given frequency at different phase shifts θ

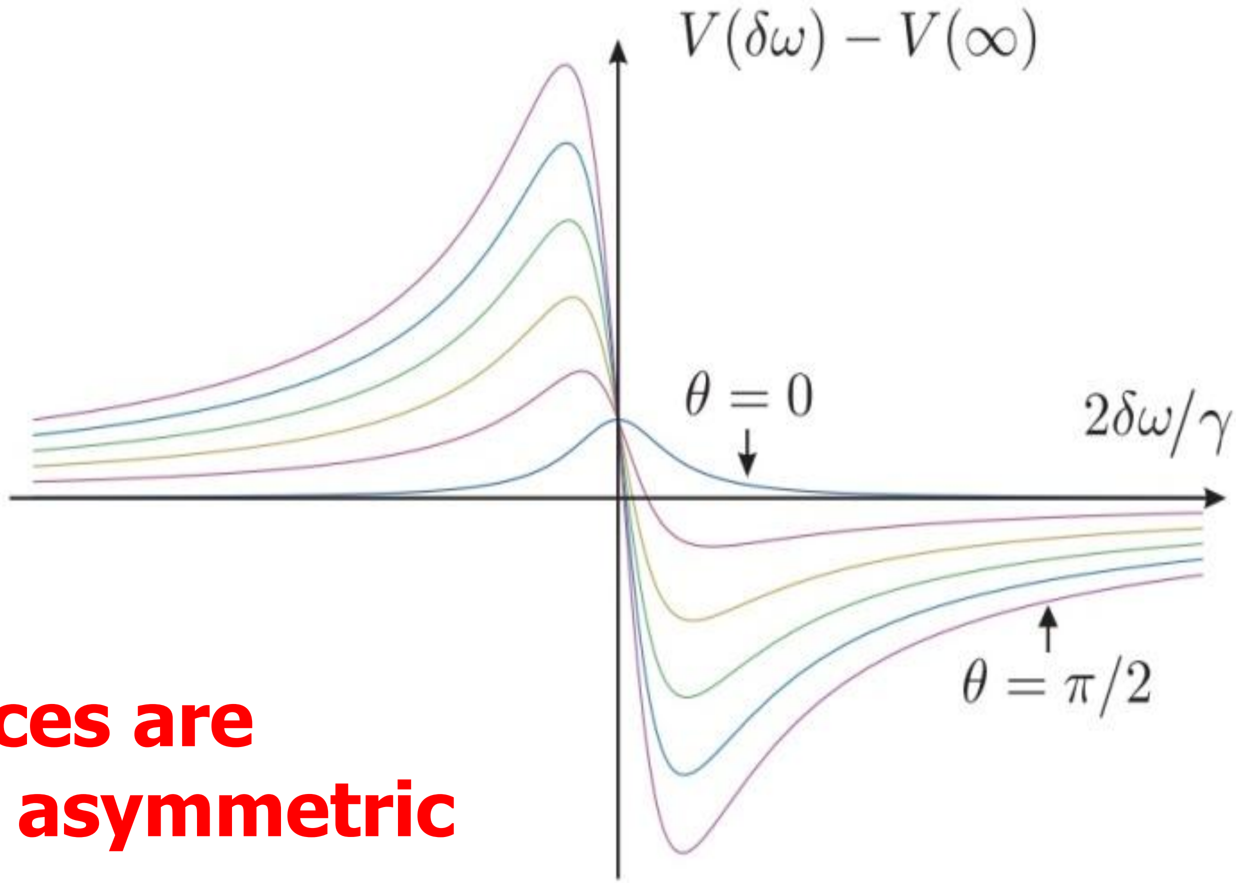

resonances are strongly asymmetric

Limiting cases: high-frequency regime

$$\omega_0 \ll \gamma \ll \omega, \quad k = \frac{\Omega + i\Gamma}{s} = \frac{\omega + i\gamma/2}{s}$$

$$V_{dc} = \frac{3({U_a}^2 - {U_b}^2)}{4U_g} + \frac{4U_a U_b e^{-\gamma L/2s}\sin(\pi\omega/\omega_0)\sin\theta}{U_g}$$

periodic oscillations with frequency

Limiting cases: high-frequency regime

$$\omega_0 \ll \gamma \ll \omega, \quad k = \frac{\Omega + i\Gamma}{s} = \frac{\omega + i\gamma/2}{s}$$

$$V_{\boldsymbol{dc}} = \frac{3({U_a}^2 - {U_b}^2)}{4U_g} + \frac{4U_a U_b e^{-\gamma L/2s} \sin(\pi\omega/\omega_0) \sin\theta}{U_g}$$

periodic oscillations with frequency

Homodyne detector operation scheme

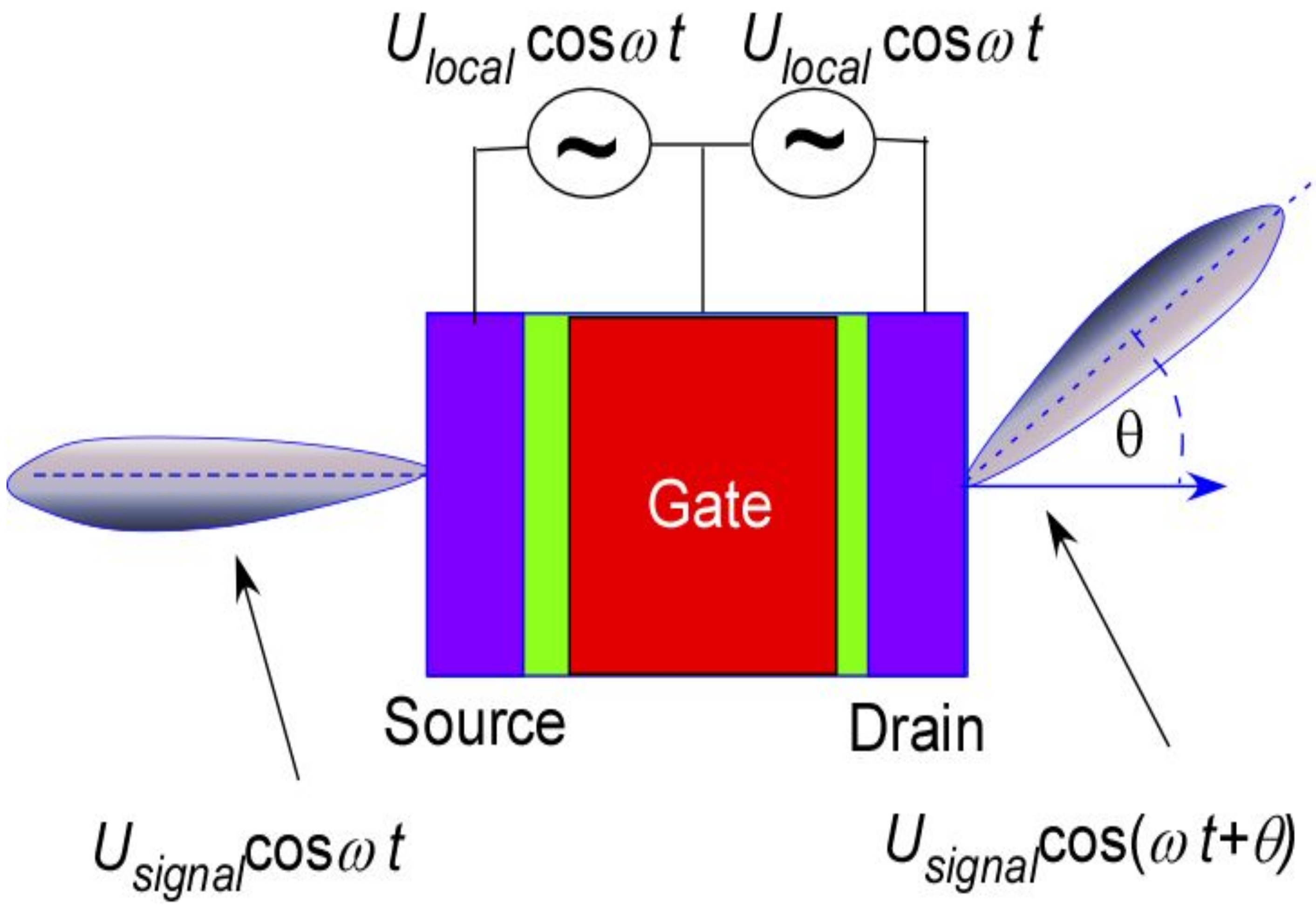

Heterodyne operation scheme

Strong local oscillator U_{local} + weak phase-asymmetric signal U_{signal}

$$U_{local} \gg U_{signal}$$

$$U(0) = U_{local}\cos\omega t + U_{signal}\cos\omega t$$
$$U(L) = U_{local}\cos\omega t + U_{signal}\cos(\omega t + \theta)$$

⟷

$$U(0) = U_a\cos\omega t$$
$$U(L) = U_b\cos(\omega t + \tilde{\theta})$$

$$\theta = 0 \rightarrow response = 0$$

$$U_a = U_{local} + U_{signal}$$
$$U_b e^{i\tilde{\theta}} = U_{local} + U_{signal}\,e^{i\theta}$$

$$U_a{}^2 - U_b{}^2 = 2U_{local}U_{signal}(1-\cos\theta) \rightarrow symmetric\ part$$
$$U_aU_b\sin\tilde{\theta} \approx U_{local}U_{signal}\sin\theta \rightarrow asymmetric\ part$$

Response of Homodyne detector

$$V \approx \frac{U_{local} U_{signal}}{2U_g} \frac{(3\gamma^2/4 - \delta\omega^2)(1-\cos\theta) + 2(-1)^{\mathrm{N}}\gamma\delta\omega\sin\theta}{(\delta\omega^2 + \gamma^2/4)}.$$

Response of Homodyne detector

Response

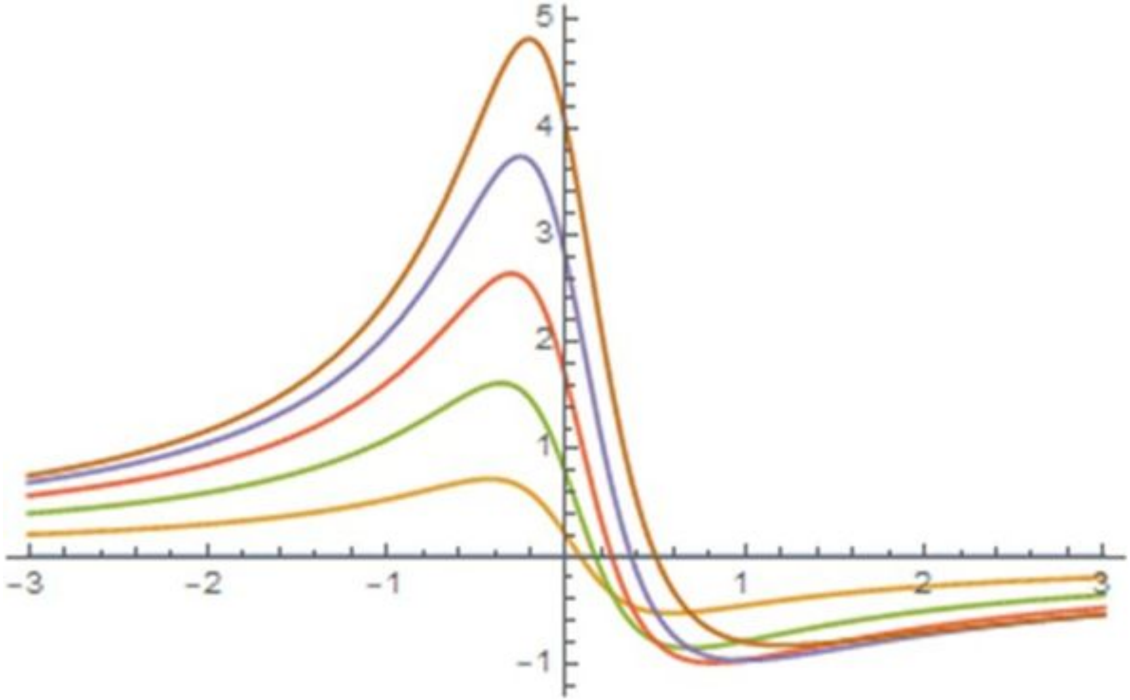

Δω/γ

Materials parameters

Material	Parameters	
	Effective mass	Mobility (m^2/Vs)
p-diamond	0.74	0.53
n-Si	0.19	0.10
n-GaN	0.24	0.15
n-InGaAs	0.041	0.8

Diamond TeraFET response normalized to U_a^2 for L=250 nm (a), 130 nm (b), 65 nm (c) and 25nm (d)

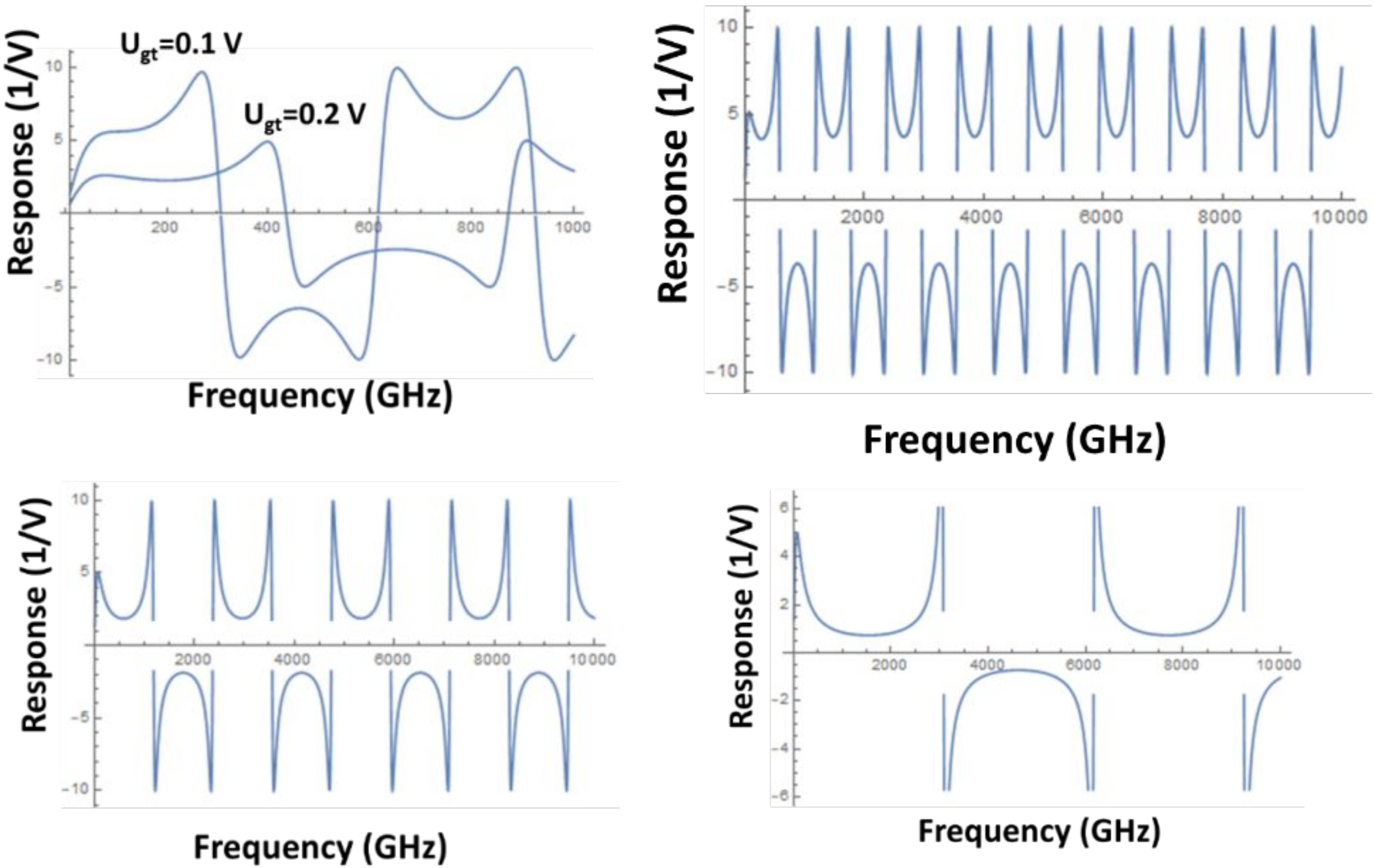

Silicon TeraFET response normalized to U_a^2 for L=130 nm (a), 65 nm (b) and 25nm (c)

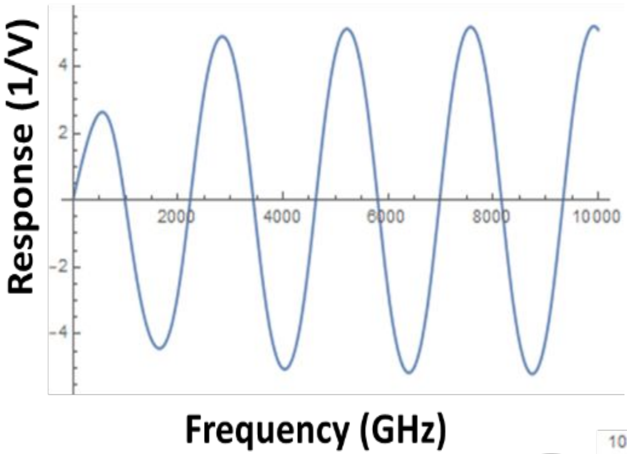

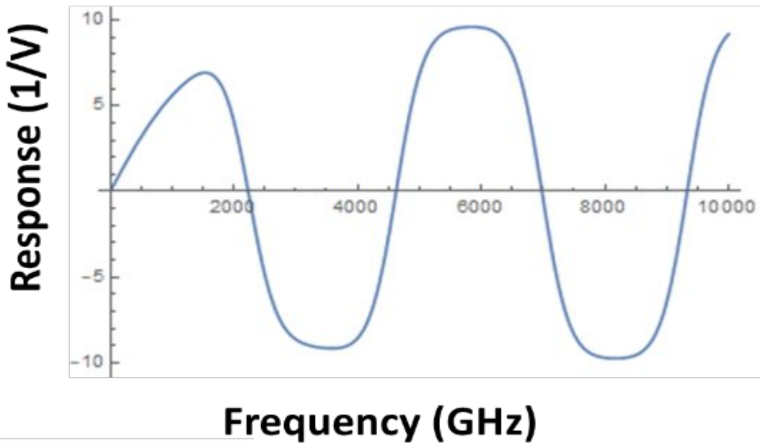

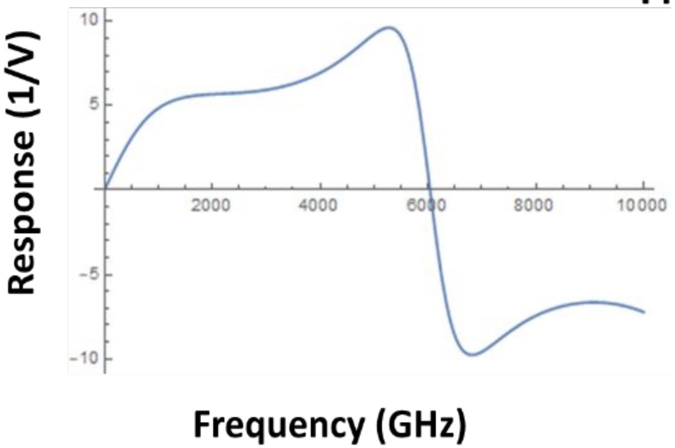

AlGaN/GaN TeraFET response normalized to U_a^2 for L=130 nm (a), 65 nm (b) and 25nm (c)

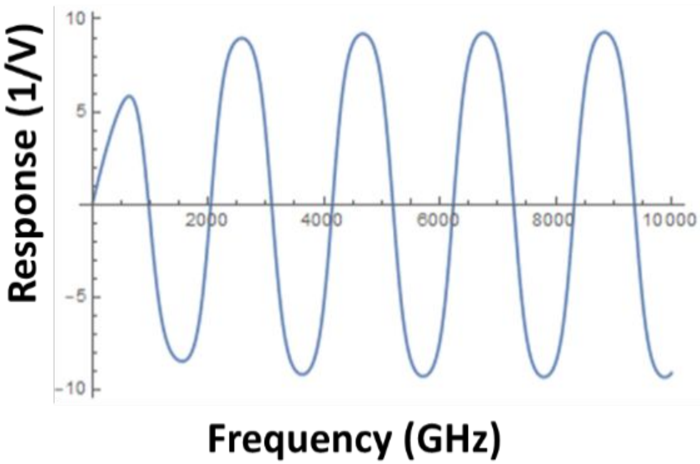

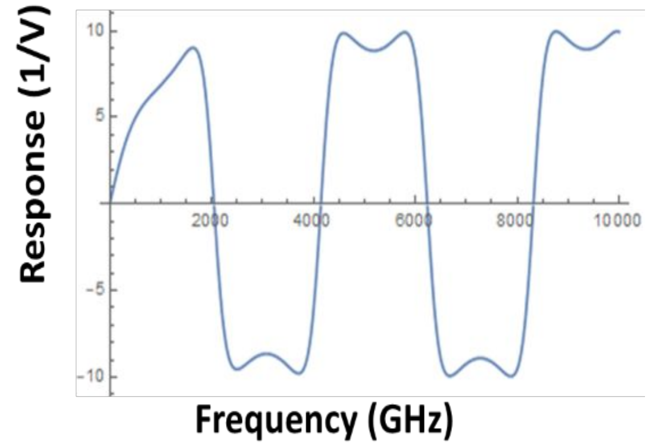

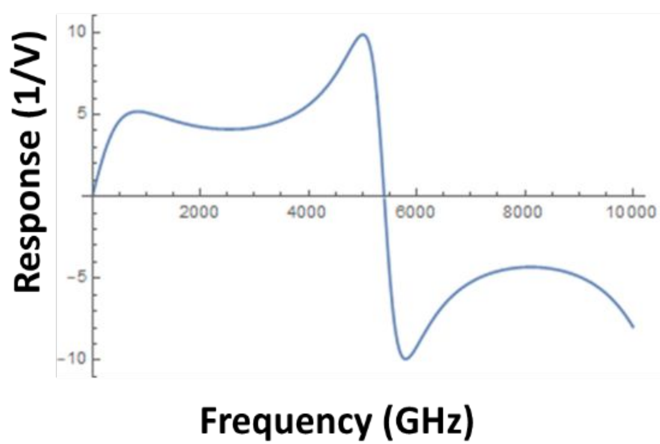

Conclusions

- Phase-asymmetry-induced dc photoresponse in the FET subjected to THz radiation leads to sharp resonant peaks in vicinity of plasmonic resonances.
- The peaks have asymmetric shape as a function of frequency.
- Homodyne detection using phase asymmetry increases sensitivity by orders of magnitude
- These results can be used for creation compact, tunable spectrometers of THz radiation

Acknowledgment

This work was made possible by Army Research Laboratory under ARL MSME Alliance (Project Manager Dr. Meredith Reed), by Army Research Office (Program Manager Dr. Joe Qiu) and by Office of Naval Research (Project Manager Dr. Paul Maki)

Special thanks to NRL for 2018 Distinguished Faculty Summer Fellowship